Ab initio investigation of the elastic properties of Ni_3Fe

Guisheng Wang,[1] Qing-Miao Hu,[2] Kalevi Kokko,[3,4] Börje Johansson,[1,5] and Levente Vitos[1,5,6]

[1]*Applied Materials Physics, Department of Materials Science and Engineering, Royal Institute of Technology, Stockholm SE-100 44, Sweden*

[2]*Shenyang National Laboratory for Materials Science, Institute of Metal Research, Chinese Academy of Sciences, 72 Wenhua Road, Shenyang 110016, China*

[3]*Department of Physics and Astronomy, University of Turku, FI-20014 Turku, Finland*

[4]*Turku University Centre for Materials and Surfaces (MatSurf), Turku, Finland*

[5]*Department of Physics and Astronomy, Division of Materials Theory, Uppsala University, Box 516, SE-75121 Uppsala, Sweden*

[6]*Research Institute for Solid State Physics and Optics, Wigner Research Center for Physics, P. O. Box 49, H-1525 Budapest, Hungary*

(Received 8 October 2013; published 27 November 2013)

Ab initio alloy theory, formulated within the exact muffin-tin orbitals method in combination with the coherent-potential approximation, is used to determine the elastic properties of Ni-Fe alloys with Fe:Ni ratio 1:3. The interplay between magnetic and chemical effects is investigated by computing the lattice parameters and the single- and polycrystal elastic moduli for different partially ordered structures in the ferro- and paramagnetic states. It is found that the influence of long-range chemical order on the bulk properties strongly depends on the magnetic state. The largest magnetic-order-induced changes are obtained for the chemically ordered $L1_2$ phase. The ferromagnetic $L1_2$ system possesses ∼5.4% larger elastic Debye temperature than the paramagnetic $L1_2$ phase, which in turn has a similar Θ_D as the chemically disordered face-centered cubic phase in either the ferro- or paramagnetic state. It is concluded that magnetic ordering has a substantially larger impact on the bulk parameters of Ni_3Fe than chemical ordering. The calculated trends are explained based on the electronic structure of nonmagnetic, ferromagnetic, and paramagnetic ordered and disordered phases.

DOI: 10.1103/PhysRevB.88.174205 PACS number(s): 63.50.−x, 71.15.Nc, 62.20.de, 71.20.Be

I. INTRODUCTION

Due to its high permeability, the nickel-rich Fe-Ni Permalloy finds applications in a number of magnetic devices. When the concentration of Ni is close to 75 at.%, the Fe-Ni system tends to order at low temperatures, which produces perceptible changes in the elastic properties,[1,2] lattice parameters,[3] specific-heat capacity,[4] resistivity,[5,6] and not least in permeability and magnetostriction.[7] In order to retain favorable magnetic properties, alloying with other elements was considered with the aim of suppressing the precipitation of the ordered phase.[7]

The stoichiometric Ni_3Fe undergoes a second-order paramagnetic-ferromagnetic transition at $T_C = 870$ K and a first-order transition from a disordered face-centered cubic to an ordered $L1_2$ phase at $T_o = 780$ K. The fact that the two transition temperatures are close to each other suggests a strong interplay between the chemical and magnetic terms. Himuro *et al.*[5] reported that the magnetic ordering increases the stability of the $L1_2$ phase, and the chemical ordering stabilizes the ferromagnetic state. The complex magnetochemical effects make the exploration of the physical properties of the Ni_3Fe alloy difficult for both experiment and theory. The ordering transition in Ni_3Fe is very slow even when the temperature is far below the critical point, which limits the available experimental data for the perfectly ordered Ni_3Fe system. Recently, the effect of chemical ordering on the lattice parameter of Ni_3Fe was studied using the ball milling method. It was found that the lattice parameter changes from ∼3.564 to ∼3.585 Å upon chemical disordering.[8] This change is, however, much larger than that from earlier measurements.[6,9,10] The specific heat of Ni_3Fe was measured in the temperature range 1.2–4.4 K,[4] and the results showed that the heat capacity decreases by ∼30% and the Debye temperature increases by ∼1.7% (∼7.8 K) on ordering.

Understanding and describing the Permalloy requires careful investigations which can properly account for both chemical and magnetic effects. In spite of the large number of works, the impact of magnetochemical ordering on the elastic parameters of Ni_3Fe has rarely been reported. The aim of our work is to fill this gap. To this end, we adopt first-principles tools well suited to study the elastic properties of ferromagnetic and paramagnetic Ni_3Fe alloys with various degrees of chemical order. In particular, we employ the exact muffin-tin orbitals method[11–14] in combination with the coherent-potential approximation[15,16] to model the partially ordered and disordered phases of Ni_3Fe. This theoretical approach has been proven to be an appropriate tool to reveal small ordering-induced changes in the elastic parameters.[17,18] From the present results obtained for the Ni-Fe system, we conclude that, although the chemical long-range order has a measurable impact on the elastic parameters, the magnetic ordering produces significantly larger changes in the bulk parameters especially in the chemically ordered $L1_2$ phase.

The rest of the paper is divided into three main sections and the conclusions. Section II gives a brief overview of the theoretical methodology, the basics of the elastic constant calculations, and the numerical details. The results are presented in Sec. III. Here, using the limited number of available theoretical and experimental data on the Ni_3Fe system, we also assess the accuracy of the present theoretical approach. The trends obtained are discussed and explained in Sec. IV.

II. THEORETICAL TOOLS

A. Total energy method

All total energy calculations were performed using the exact muffin-tin orbitals (EMTO) method.[11–14] This density

functional solver is an improved screened Korringa-Kohn-Rostocker method, where the exact Kohn-Sham potential is represented by large overlapping potential spheres. Inside these spheres the potential is spherically symmetric and constant between the spheres. It was shown[19,20] that using overlapping spheres gives a better representation of the full potential as compared to the traditional muffin-tin or atomic-sphere approximations. Within the EMTO method, the compositional and magnetic disorder is treated using the coherent-potential approximation[15,16] (CPA) and the total energy is computed via the full charge-density technique.[21–23] The EMTO-CPA method has been involved in many successful applications focusing on the thermophysical properties of alloys and compounds.[11–14,17,18,24–27]

B. Elastic properties

The elastic properties of a single crystal are described by the elements of the elasticity tensor. In a cubic lattice, there are three independent elastic constants: C_{11}, C_{12}, and C_{44}. The tetragonal shear elastic constant (C') and the bulk modulus (B) are connected to the single-crystal elastic constants as $B = \frac{1}{3}(C_{11} + 2C_{12})$ and $C' = \frac{1}{2}(C_{11} - C_{12})$. The adiabatic elastic constants are defined as the second-order derivatives of the energy (E) with respect to the strain tensor. Accordingly, the most straightforward way to obtain the elastic parameters is to strain the lattice and evaluate the total energy change as a function of lattice distortion. In practice, the bulk modulus and the equilibrium volume (V) are derived from the equation of state, obtained by fitting the total energy data calculated for seven different cubic lattice constants (a) by a Morse type of function.[28] Since the total energy depends on volume much more strongly than on small lattice strains, volume-conserving distortions are usually more appropriate to calculate C' and C_{44}. Here, we employ the following orthorhombic (D_o) and monoclinic (D_m) deformations:

$$D_o = \begin{pmatrix} 1+\delta_o & 0 & 0 \\ 0 & 1-\delta_o & 0 \\ 0 & 0 & \frac{1}{1-\delta_o^2} \end{pmatrix} \quad \text{and}$$

$$D_m = \begin{pmatrix} 1 & \delta_m & 0 \\ \delta_m & 1 & 0 \\ 0 & 0 & \frac{1}{1-\delta_m^2} \end{pmatrix}, \tag{1}$$

respectively, applied on the unstrained conventional cubic unit cell. These deformations lead to total energy changes $\Delta E(\delta_o) = 2VC'\delta_o^2 + O(\delta_o^4)$ and $\Delta E(\delta_m) = 2VC_{44}\delta_m^2 + O(\delta_m^4)$, respectively, where O stands for the neglected terms.

The polycrystalline shear modulus (G) is obtained from the single-crystal data according to the Hill averaging $G = (G_V + G_R)/2$ of the Voigt, $G_V = (C_{11} - C_{12} + 3C_{44})/5$, and Reuss, $G_R = 5(C_{11} - C_{12})C_{44}/[4C_{44} + 3(C_{11} - C_{12})]$, bounds. Finally, the elastic Debye temperature

$$\Theta_D = \frac{\hbar}{k_B}\left(\frac{18\pi^2}{V}\right)^{1/3}\left(\frac{1}{v_L^3} + \frac{2}{v_T^3}\right)^{-1/3} \tag{2}$$

($\hbar$ and k_B are the reduced Planck constant and the Boltzmann constant, respectively) is derived from the longitudinal (v_L) and the transverse (v_T) sound velocities obtained from the polycrystalline elastic moduli and density (ρ), viz., $v_L = \sqrt{(B + 4G/3)/\rho}$ and $v_T = \sqrt{G/\rho}$.

C. Transition temperature

In the completely disordered Ni_3Fe system, the fcc sites are occupied by Ni and Fe atoms with probabilities 3/4 and 1/4 respectively; in the ordered $L1_2$ structure, the corner sites are occupied by Fe and the face-center sites by Ni. The order-disorder transition temperature (T_o) can be estimated using the Bragg-Williams-Gorsky approximation.[29] According to that, the degree of order $S \equiv (p - r)/(1 - r)$ may be expressed as

$$S(U,T) = 1 - \frac{[4r(1-r)(e^x - 1) + 1]^{1/2} - 1}{2r[1 - r(e^x - 1)]},$$
$$x = U/k_BT, \tag{3}$$

where r is the concentration of Fe atoms in the system, p is the probability of finding an Fe atom on the corner site, T is the temperature, and U is an average increment in the potential energy when one Fe atom is interchanged with a Ni atom. Assuming a linear relationship between the order parameter and the energy cost U, viz., $U = U_0S$, where U_0 is the maximum interchange energy corresponding to $S = 1$, one can solve Eq. (3) for a given T. For the critical temperature of the order-disorder transition (where S vanishes) we get $T_o \approx 0.21U_0/k_B$.

We should mention that U_0 describes the completely ordered $L1_2$ structure. This energy is obtained by interchanging a small fraction (typically around 0.1 at. %) of Fe atoms from the corner site with the Ni atoms at the face-centered sites. Since in the present approach the noninteger site occupations are treated within the single-site mean-field coherent-potential approximation, the above interchange energy is unambiguously defined. In other words, U_0 does not contain any local environment (short-range-order) effects.

D. Details of numerical calculations

Previous studies show that usually the effect of chemical long-range order on the elastic constants is very small.[17,18] In order to be able to resolve such small differences and obtain curves with the proper tendency, one needs to pay special attention to the numerical accuracy of the calculations. In the present electronic structure and total energy calculations, the one-electron equations were solved within the all-electron soft-core scheme and using the scalar-relativistic approximation (taking into account the mass-velocity and Darwin terms). The Green's function was calculated for 16 complex energy points distributed exponentially on a semicircular contour including states within 1 Ry below the Fermi level. In the basis set, we included s, p, d, and f orbitals and in the one-center expansion of the full charge density $l_{\max} = 8$ was used. The total energy was evaluated by the shape function technique with $l_{\max}^{\text{shape}} = 30$.[14] For the undistorted $L1_2$ structure, we found that a homogeneous k mesh of $29 \times 29 \times 29$ ensured the required accuracy. For the orthorhombic and monoclinic structures, the k mesh was set to $15 \times 15 \times 15$ and $15 \times 29 \times 21$ in the corresponding irreducible Brillouin zones. For both lattice distortions, six strains $\delta = 0, 0.01, 0.02, \ldots, 0.05$ were used. All potential

sphere radii were fixed to the average Wigner-Seitz radius. The self-consistent EMTO calculations were performed within the generalized gradient approximation proposed by Perdew, Burke, and Ernzerhof (PBE),[30] which has been verified for the Fe-Ni-based systems by many former investigations.[31–33]

In the ordered $L1_2$ structure, there are three Ni atoms at the face-center positions and one Fe atom located at the origin. In partially ordered structures, the degree of long-range order was controlled by changing the composition at the face-center positions as $Ni_{1-x}Fe_x$ and at the origin as $Ni_{3x}Fe_{1-3x}$, represented by the formula unit $(Ni_{1-x}Fe_x)_3(Ni_{3x}Fe_{1-3x})$. Accordingly, we changed x from 0 (corresponding to Ni_3Fe in the $L1_2$ structure) to 0.25 (corresponding to the completely disordered $Ni_{0.75}Fe_{0.25}$ alloy in the fcc structure). Hence, the degree of disorder may be expressed as $S = 1 - 4x$.

The paramagnetic state was modeled via the disordered local magnetic moment (DLM) picture.[34] Accordingly, we used the configuration $(Ni^{\uparrow}_{n/2}Ni^{\downarrow}_{n/2})(Fe^{\uparrow}_{f/2}Fe^{\downarrow}_{f/2})$, f being the concentration of Fe and n that of Ni at a given site (e.g., $f = 1 - 3x$ and $n = 3x$ for the site at the origin) and the arrow showing the magnetic moment of the atoms. The DLM approach has been widely used to model systems well above the magnetic transition temperature (i.e., in the fully disordered paramagnetic state).

The impurity problem is solved within the single-site (CPA) approximation, and hence the Coulomb system of a particular alloy component i may contain a nonzero net charge. In the present application, the effect of charge misfit was taken into account using the screened-impurity model (SIM).[35,36] According to that, the additional shift in the one-electron potential and the corresponding correction to the total energy are controlled by the dimensionless screening parameters α_i and β. The parameters α_i are determined from the average net charges and electrostatic potentials of the alloy components obtained in regular supercell calculations.[36] The second dimensionless parameter β is determined from the condition that the total energy calculated within the CPA should match the total energy of the alloy obtained using the supercell technique. For most alloys, the suggested optimal values of β and α_i are between ~0.6 and ~1.2.[35,36] Often, the SIM parameters α_i and $\alpha \equiv \beta\alpha_i$ are chosen to be the same.[14]

In order to get a suitable SIM parameter for the Ni_3Fe system, we made use of a special quasirandom structure[37,38] (SQS) containing 16 atoms per unit cell and computed the total energy for four different lattice parameters (a = 3.4665, 3.5207, 3.5748, and 3.6290 Å) using the EMTO method. Then we compared the SQS total energy to that obtained by the CPA using different SIM parameters. For this optimization, we adopted the PBE functional and for the sake of simplicity we assumed $\alpha_i = \alpha$. The results are summarized in Fig. 1, which shows that the optimal SIM parameter weakly depends on the lattice parameter. In contrast to Cu_3Au, where the SIM parameters are somewhat more sensitive to the volume,[18] here we find that ~0.9 is a good choice for the optimal α value in Ni_3Fe irrespective of the volume. In the following, all calculations are based on $\alpha = \alpha_i = 0.9$.

III. RESULTS

The calculated bulk properties of ferromagnetic (FM) and paramagnetic (PM) Ni_3Fe are shown in Figs. 2–7. For

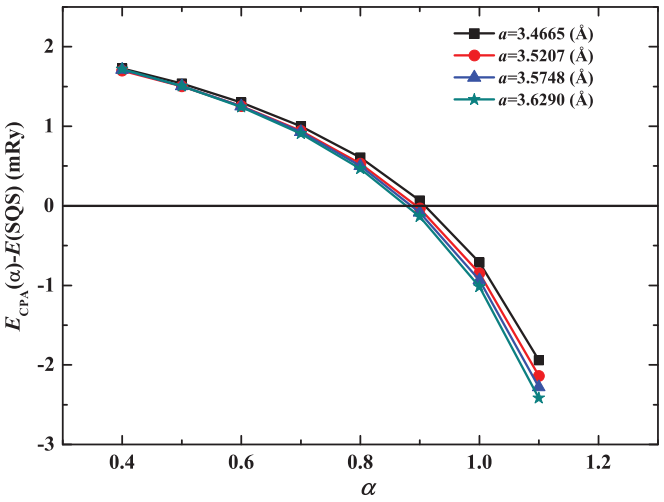

FIG. 1. (Color online) Total energy of fcc Ni_3Fe random alloy calculated using the EMTO-CPA method as a function of the SIM parameter α. The energies are plotted relative to the total energy of an SQS supercell containing 16 sites. Results are shown for four different lattice constants.

reference, the elastic parameters are also listed in Table I as a function of the long-range-order parameter S. We estimated the errors associated with the numerical parameters of the calculations and the numerical fittings and found that for the lattice parameters and elastic constants the error bars are below 10^{-3} Å and 0.5 GPa, respectively.

A. Equilibrium volume and magnetic moment

The total and partial magnetic moments for Fe and Ni sites in Ni_3Fe are displayed in Fig. 2 as a function of S. The present results for the ferromagnetic state agree well with the former theoretical[39] and experimental[40] values. According to

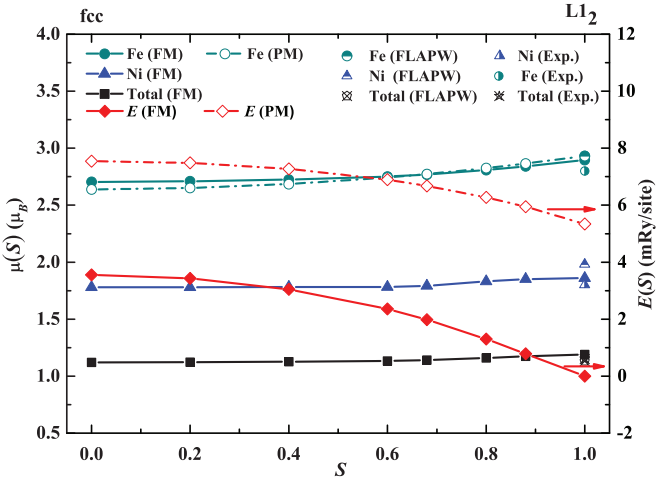

FIG. 2. (Color online) Total and partial magnetic moments in the ferromagnetic (FM) and local (Fe) magnetic moment in the paramagnetic (PM) Ni_3Fe alloys as a function of the degree of order S. The corresponding total energies per atom are shown on the right axis. The former theoretical results were obtained by the full-potential augmented plane wave (FLAPW) method (Ref. 39) and the experimental data refer to the ferromagnetic state (Ref. 40).

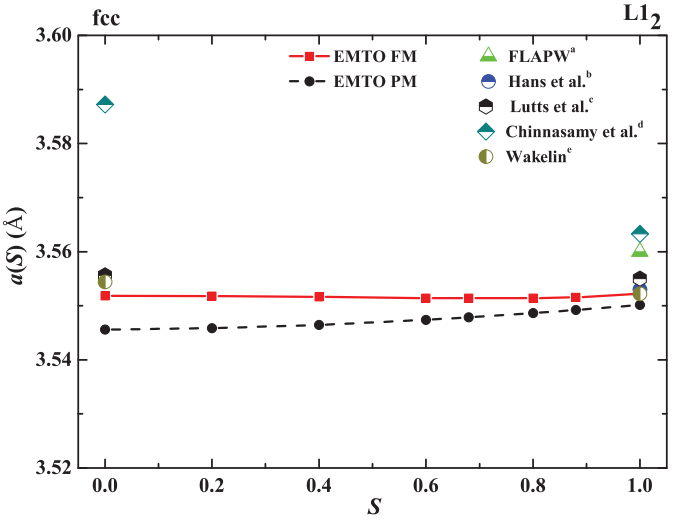

FIG. 3. (Color online) Lattice parameter as a function of the degree of the long-range order S for the ferromagnetic and paramagnetic states of Ni_3Fe. The experimental results are from Refs. 9 (*b*), 10 (*c*), 8 (*d*), and 6 (*e*). The quoted theoretical value (FLAPW) for the ordered ferromagnetic state is from Ref. 39 (*a*). All experimental results refer to the ferromagnetic state.

the present findings, in the FM state the magnetic moments of Fe (Ni) atoms increase from $\sim 2.7\mu_B$ ($\sim 1.7\mu_B$) to $\sim 2.9\mu_B$ ($\sim 1.9\mu_B$) with increasing long-range order. We notice that the Ni moments vanish in the PM (DLM) state, but the Fe local magnetic moments are very similar for the two magnetic states.

Figure 2 also shows that the total energy $E(S)$ plotted as a function of the degree of order S decreases as the system becomes chemically more ordered. The energy difference between paramagnetic and ferromagnetic states increases from ~ 4 mRy to ~ 5.3 mRy when the long-range-order parameter

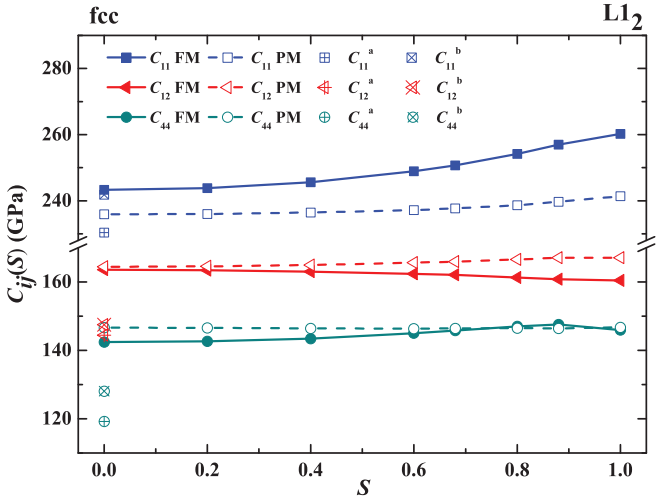

FIG. 4. (Color online) Single-crystal elastic constants C_{11}, C_{12}, and C_{44} plotted as a function of the degree of order S for the ferromagnetic and paramagnetic states of Ni_3Fe. For comparison, we included the available experimental data for $Ni_{77.82}Fe$ from Ref. 1 (*a*) (room-temperature data) and $Ni_{79.19}Fe$ from Ref. 2 (*b*) (extrapolated from lower-temperature values to 0 K). All experimental results refer to the ferromagnetic state.

changes from 0 to 1. This implies that chemical ordering stabilizes the ferromagnetic order with respect to the PM state.

In Fig. 3, we compare our results for the lattice parameter a with the experimental values[6,8–10] and the previous theoretical result.[39] The present result for the chemically ordered $L1_2$ phase turns out to be in good agreement with most of the experimental data. We also notice that on the average the agreement with experiments is better for the EMTO results than for the full-potential augmented plane wave (FLAPW) results.[39] Comparing the quoted experimental values, we observe that the milling method slightly overestimates the lattice parameter as compared to the other values. Chinnasamy *et al.*[8] reported lattice parameters between 3.563 and 3.587 Å, depending on the milling time (only the smallest value is shown in Fig. 5). They argue that the somewhat larger lattice parameter compared to other experimental results is due to the disordering created upon milling. This speculation might seem to fail in light of the present study. Even if there is such a lattice expansion effect with decreasing chemical order parameter, that should be much smaller than the one seen in Ref. 8. On the other hand, we should point out that the present theory cannot account for the grain-boundary and other extended defects created by milling, which may be another plausible reason for the above discrepancy.

For the ferromagnetic state of Ni_3Fe, we find that the lattice parameter change is less than 10^{-3} Å, which can in fact be ignored within the present estimated error bar associated with the numerical fit of the equation of state. For the paramagnetic state, the lattice parameter change due to ordering is 4.5×10^{-3} Å. This change is slightly larger than the one obtained for the ferromagnetic state, and it might have some effect on the volume-sensitive physical properties. Magnetism mainly affects the lattice parameter in the random solid solution, and this effect almost disappears as the system approaches the ordered state.

It is interesting to note that according to the present calculations, the lattice parameter slightly increases (4.5×10^{-3} Å) when going from the chemically and magnetically disordered state to the ordered state. This is against common expectations. Namely, the lattice parameter should shrink with increasing degree of order as is found for most materials.[3] That is because ordered systems have stronger bonds which should be reflected by higher density. Furthermore, as we will see in the next section, some of the elastic constants also increase with S. Usually a larger lattice parameter corresponds to a smaller elastic constant (i.e., the third-order elastic constants are negative). This observation makes the anomalous behavior of the lattice parameter even more interesting. Although the above change in a is extremely small, it calls for further investigations from both the theoretical and experimental sides.

B. Disorder effect on the elastic constants

The calculated single-crystal elastic constants C_{11}, C_{12}, and C_{44} are plotted in Fig. 4 as functions of the long-range-order parameter S for the ferromagnetic and paramagnetic states. Before discussing the trends obtained, we assess the accuracy of our results. As there are no experimental single-crystal elastic constants for the stoichiometric ordered and disordered structures, we make comparisons with the available data for

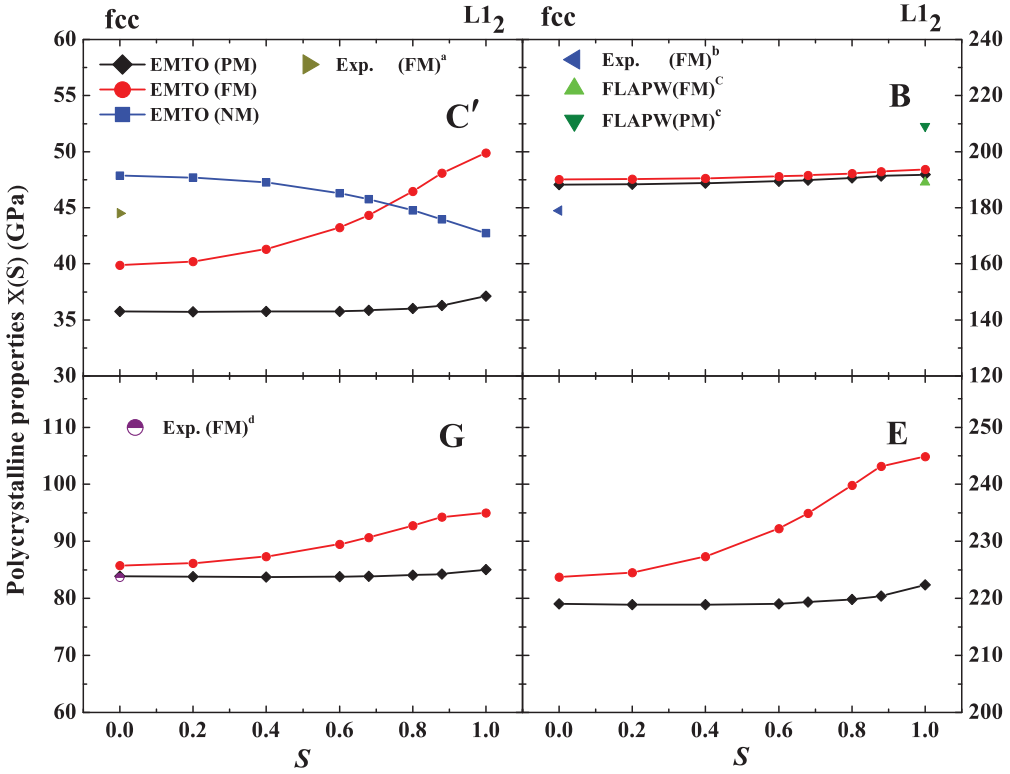

FIG. 5. (Color online) The tetragonal shear elastic constant (C') and polycrystalline elastic moduli (B, G, and E) as functions of the degree of order S for the ferromagnetic and paramagnetic states of Ni_3Fe. For reference (see the text), C' values obtained for the hypothetical nonmagnetic (NM) systems are also shown. For comparison, the values from Ref. 41 (*a*), Ref. 42 (*b*), Ref. 39 (*c*), and Ref. 42 (*d*) are shown.

$Ni_{77.82}Fe$ and $Ni_{79.19}Fe$. Since the composition ratio is not exactly 1:3, at low temperatures these two systems should be a mixture of ordered and disordered phases. Not knowing the degree of order S for these two systems, we plot all of the experimental values referred to in the left side of the figure (at $S = 0$), but keep in mind that these values do not correspond to fully disordered states. Taking into account that temperature (neglected in the present study), chemical composition, and degree of order all affect the elastic parameters, we might conclude that the results from the EMTO calculations are in line with the quoted experimental values.

Figure 4 shows that in the ferromagnetic state, C_{11} increases by 8.3% with increasing S. At the same time, C_{12} slightly decreases and C_{44} increases with S. However, these latter changes are substantially smaller in absolute value than that

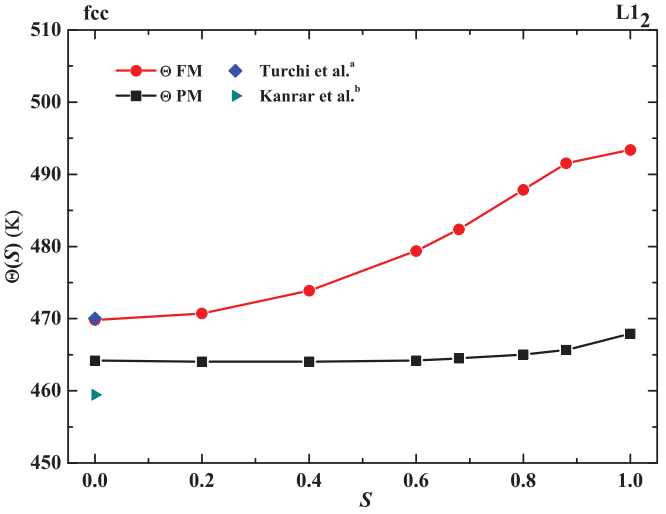

FIG. 6. (Color online) The Debye temperature as a function of the degree of order S for the ferromagnetic and paramagnetic states of Ni_3Fe. The available experimental data are from Ref. 43 (*a*) and Ref. 2 (*b*) for $Ni_{79.19}Fe$.

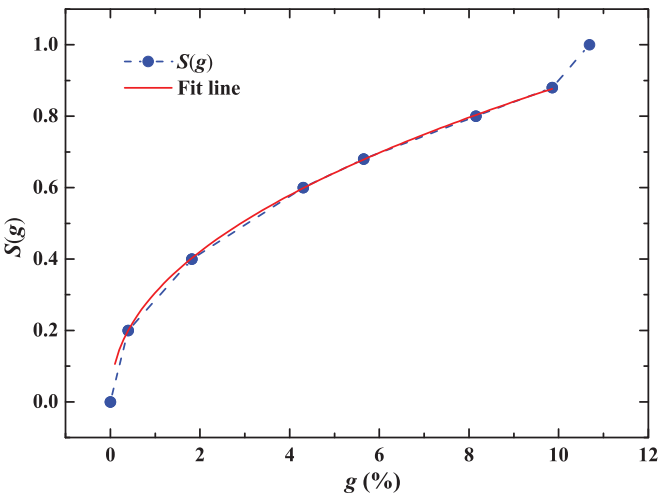

FIG. 7. (Color online) The degree of order S plotted as a function of $g \equiv (G - G_d)/G_d$, where G is the partially ordered and G_d the fully disordered shear modulus.

TABLE I. Theoretical single-crystal elastic constants $C_{11}(S)$, $C_{12}(S)$, $C_{44}(S)$, and $C'(S)$, polycrystalline bulk $B(S)$, shear $G(S)$, and Young's $E(S)$ moduli (GPa), Poisson's ratio ν, Pugh ductile/brittle ratio B/G, Zener anisotropy ratio C_{44}/C', Cauchy pressure $(C_{12}-C_{44})$ (GPa), and Debye temperature Θ_D (K) for ferromagnetic (upper panel) and paramagnetic (lower panel) Ni_3Fe alloys as a function of the degree of order S. The estimated error bar for the elastic parameters is below 0.5 GPa.

S	B	C'	C_{11}	C_{12}	C_{44}	G	E	ν	Θ_D	$(C_{12}-C_{44})$	C_{44}/C'	B/G
						Ferromagnetic Ni_3Fe						
1	193.7	49.9	260.2	160.4	145.9	95.0	244.9	0.289	493.4	14.51	2.92	2.04
0.88	192.8	48.1	256.9	160.8	147.6	94.3	243.2	0.290	491.6	13.21	3.07	2.05
0.8	192.3	46.5	254.2	161.3	147.0	92.8	239.8	0.292	487.8	14.26	3.16	2.07
0.68	191.6	44.3	250.7	162.0	145.8	90.7	234.9	0.296	482.4	16.27	3.29	2.11
0.6	191.2	43.3	248.9	162.4	145.0	89.5	232.2	0.298	479.4	17.42	3.35	2.14
0.4	190.5	41.3	245.6	163.0	143.4	87.4	227.3	0.301	473.9	19.53	3.47	2.18
0.2	190.2	40.2	243.8	163.4	142.6	86.1	224.5	0.303	470.7	20.81	3.55	2.21
0	190.1	39.9	243.3	163.5	142.4	85.8	223.7	0.304	469.8	21.12	3.57	2.22
						Paramagnetic Ni_3Fe						
1	193.7	37.1	243.2	168.9	146.7	85.1	222.6	0.308	468.0	22.19	3.95	2.28
0.88	191.3	36.3	239.7	167.1	146.5	84.3	220.5	0.308	465.8	20.54	4.04	2.27
0.8	190.6	36.0	238.6	166.6	146.4	84.0	219.8	0.308	464.9	20.18	4.07	2.27
0.68	189.9	35.9	237.7	166.0	146.3	83.8	219.3	0.308	464.4	19.65	4.08	2.27
0.6	189.5	35.8	237.2	165.6	146.3	83.8	219.0	0.307	464.1	19.34	4.09	2.26
0.4	188.8	35.7	236.4	165.0	146.4	83.8	218.9	0.307	464.0	18.57	4.10	2.25
0.2	188.4	35.7	236.0	164.6	146.5	83.8	218.9	0.306	464.0	18.04	4.10	2.25
0.0	188.2	35.8	235.9	164.4	146.6	83.8	219.0	0.306	464.1	17.84	4.02	2.25

of C_{11}. In the paramagnetic state, all elastic constants remain almost constant as a function of S. That is, the single-crystal elastic constants are not affected by the degree of long-range order in the magnetically disordered state. This finding is in accordance with the results reported for the nonmagnetic Cu_3Au (Ref. 18) and $Pd_{0.5}Ag_{0.5}$ (Ref. 17) alloys. Therefore, different magnetic states lead to markedly different behavior of the elastic constants as a function of the long-range chemical order.

On the other hand, different degrees of chemical order produce quite different dependence of the single-crystal elastic constants on the magnetic state. In particular, C_{11} and C_{12} have much bigger responses to the magnetic ordering effect in the chemically ordered state than in the disordered state. But C_{44} behaves in the opposite way; it has a bigger response to the magnetic effect in the chemically disordered state. When $S \lesssim 0.4$, the magnetic effect on C_{12} may be ignored, but it has sizable impact on C_{44}. When $S \gtrsim 0.4$, the magnetic effect in C_{12} becomes important, but C_{44} keeps almost the same value for the two magnetic states.

The tetragonal shear elastic constant $C' = (C_{11} - C_{12})/2$ is shown in the left upper corner of Fig. 5 along with one experimental value reported for the disordered FM state.[41] In the ferromagnetic state, C' increases by ~25% when going from the disordered to the ordered state. This change is very large, which shows that the ordered state is significantly more stable mechanically than the disordered state. In the paramagnetic state, C' changes only by ~3.6% as S increases from 0 to 1. Therefore, magnetism affects C' and thus the elastic anisotropy (C_{44}/C') in very different ways at different degrees of order. In the chemically ordered state, the magnitude of C' increases from 37.1 GPa to 49.9 GPa (~35%) upon magnetic ordering. The effect is diminished as the degree of order gradually decreases. This confirms that magnetismdynamically stabilizes the ordered state.

The polycrystalline elastic parameters are summarized in Fig. 5. The present bulk modulus B and shear modulus G are in line with the experimental and the former theoretical values in most phases. An exception is the paramagnetic $L1_2$ phase, for which the EMTO bulk modulus differs considerably from the FLAPW result, which was reported to be substantially higher (by ~20 GPa) than that of the ferromagnetic state. That is because in Ref. 39 nonmagnetic calculations were used to model the paramagnetic state, ignoring the effect of disordered local magnetic moments on the bulk properties.

In the ferromagnetic state, the Young's modulus E increases nonlinearly as the degree of order S increases. However, for the paramagnetic state, E is almost constant with S. The dependence of the shear modulus $G(S)$ on the long-range order for two different magnetic state is similar to that of $E(S)$. Close to the ordered state, the ferromagnetic Ni_3Fe is much stiffer than the paramagnetic phase. Close to the disordered state, the effect of magnetism almost disappears. The trend of the bulk modulus is totally different from those of $E(S)$ and $G(S)$. Namely, $B(S)$ has a weak dependence on the degree of the long-range order and magnetism. This may be understood from the trends of C_{11} and C_{12} in Fig. 4. The ordering-induced increase of C_{11} is to large extent canceled by the ordering-induced decrease of C_{12} in $B = (C_{11} + 2C_{12})/3$. Unfortunately, there are no measurements nor other theoretical results available of the bulk modulus for the ordered paramagnetic state. Thus, instead, we compare Ni_3Fe with the structurally similar Cu_3Au system, for which theoretical studies indicate that the bulk modulus B does not increase significantly with increasing degree of order. A similar conclusion was found in the case of $Pd_{0.5}Ag_{0.5}$ as well.[17]

In Table I, we also included the long-range-order effect on the Zener anisotropy ratio (C_{44}/C') and the ductile/brittle parameters. The values show that the elastic anisotropy changes

under the influence of long-range order and magnetism. The change is quite different for different magnetic states. For the paramagnetic state, the anisotropic ratio has almost no response to the long-range order. But for the ferromagnetic state, the anisotropy of Ni_3Fe decreases considerably with S. Therefore, the magnetic effect on the elastic anisotropy becomes larger as the degree of long-range order gets closer to 1.

For all cases, the magnitude of the Pugh ratio of B/G is much bigger than the critical value 1.75 for the ductile/brittle transition.[44] On this ground, we may conclude that the long-range order and magnetism do not affect the ductility of Ni_3Fe system. We should also mention that according to Table I, the Poisson ratio ν and the Cauchy pressure $(C_{12} - C_{44})$ change slightly and all of them are far from their critical ductile/brittle values. Hence, magnetism and the degree of order have negligible influence on the ductile/brittle properties of Ni_3Fe alloys.

C. Debye temperature

Figure 6 illustrates the relationship between the elastic Debye temperature and the magnetic and chemical long-range-order effects. Our results for Θ_D are surprisingly close to the results by Turchi *et al.*[43] and Kanrar and Ghosh,[2] both measurements obtained for $FeNi_{79.19}$. According to the dependence of the Debye temperature on the Ni concentration as obtained in Ref. 2, the Debye temperature of the ferromagnetic disordered Ni_3Fe system should be about ∼450 K, which is also close to the results of the present work. The difference between the Debye temperatures in the disordered and partially ordered states ($S = 0.69$) is reported to be 7.8 K.[4] This is in accordance with the results of the present *ab initio* calculations. Compared to the previous work on Cu_3Au,[18] the above change may be considered large. Due to the magnetic effects, the long-range order contributes more in the Ni_3Fe system than in the nonmagnetic Cu_3Au to the vibration entropy change upon ordering. In the chemically disordered state, magnetic ordering changes the Debye temperature by ∼1.2% compared to 5.4% (25.4 K) found for the ordered state.

The entropy change due to the order-disorder transition can be estimated from the present elastic Debye temperatures. According to the high-temperature expansion of the harmonic phonon entropy,[45] for the entropy change at the order-disorder transition we have $\Delta S_{ph}^{o\text{-}d} \approx 3k_B \ln \Theta_{\mathrm{D}}^{o}/\Theta_{\mathrm{D}}^{d}$. Using the present results, the theoretical $\Delta S_{ph}^{o\text{-}d}$ changes from $0.024k_B$ to $0.147k_B$ due to the magnetic effects, which indicates that magnetism strengthens the vibrational entropy effect. The reason behind this effect is that the elastic constants depend differently on the degree of order S for the two magnetic states. The Fe atoms have totally different distributions for the completely disordered and the ordered structures. In the ordered structure, the Fe atoms are in a simple cubic sub-lattice, but in the disordered structure, the Fe atoms occupy a face-centered cubic structure.

Considering the strong elastic-chemical coupling in the ferromagnetic state, we suggest that one can estimate the degree of order S using the measured elastic modulus. Figure 7 gives the relationship between the degree of order S and the reduced shear modulus g defined as $g \equiv (G - G_d)/G_d$, where G_d is the shear modulus of the fully disordered phase. We find that a simple power fit function can accurately reproduce the calculated data. For instance, the trial function $S(g) = ag^b$ with $a = 0.305\,59$ and $b = 0.460\,63$ reproduces well the $S(g)$ curve up to $g \sim 10\%$. Then one can find the actual degree of order S by measuring the shear modulus and comparing that to the fully disordered value.

To close our analysis about the long-range-order and magnetic effects on the elastic properties of Ni_3Fe, we use the first-principles energy to estimate the transition temperature using the Bragg-Williams-Gorsky approximation.[29] In the present work, we get $U_0 = 0.034\,333$ Ry which gives $T_o = 1138$ K. This value is very close to the Monte Carlo result (1030 K) of Ekholm *et al.*[46] According to the discussion in Ref. 46, when the temperature is close to the transition temperature, the magnetically ordered state is degenerate with the partially ordered magnetic state, and at the same time the lattice parameter has a corresponding change. This would apparently decrease the value of U_0 and consequently decrease the estimated transition temperature.

IV. DISCUSSION

From the results presented in the previous section, it is clear that, as a result of chemical ordering, the tetragonal shear elastic constant C'(FM) exhibits the largest relative change. In Fig. 5, we also show the results calculated for the hypothetical nonmagnetic (NM) state. It is found that the absolute values of the ordering effects for the FM and NM states are similar, but C'(NM) and C'(FM) follow opposite trends as a function of S. For comparison, C'(PM) is nearly constant with increasing S. In the following we try to understand the electronic structure origin of these differences by monitoring the electronic total densities of states (DOSs) of ordered and disordered alloys in FM, PM, and NM states.

The total densities of states for NM, FM, and PM Ni_3Fe alloys are shown in Fig. 8, the upper, middle, and lower panels, respectively. Results are shown for the ordered (left panels) and disordered (right panels) cases. In the figure, we included the DOSs for the undistorted fcc and $L1_2$ lattices (red solid curves) and also for the orthorhombic lattices obtained by applying the D_o distortion [Eq. (1)] with $\delta_o = 0.05$ (black dashed curves). We recall that this lattice distortion is used to compute C'. We observe that the large NM peak near the Fermi level (∼33–37 states/Ry) disappears in the FM and PM states, explaining the observed spontaneous spin polarization of the system in terms of the classical Stoner model. Furthermore, in the ordered FM state, the spin-up d channel is fully occupied, whereas the spin-down channel shows a local minimum near the Fermi level. This indicates a strong covalent type of bonds for the ordered FM system. The local minimum disappears in the disordered FM state, showing that this phase is thermodynamically less stable as compared to the ordered FM state. The occupied parts of the PM DOSs are very similar for the ordered and disordered cases.

Elastic distortion lowers the cubic symmetry and thus splits the degenerate E_g and T_{2g} states of the d density of states. If the degenerate states are present around the Fermi level (E_F), the symmetry lowering deformation usually decreases the one-electron energy and thus the kinetic energy of the system. That is because some of the split sub-bands move above the Fermi level and as a result the partial spectral

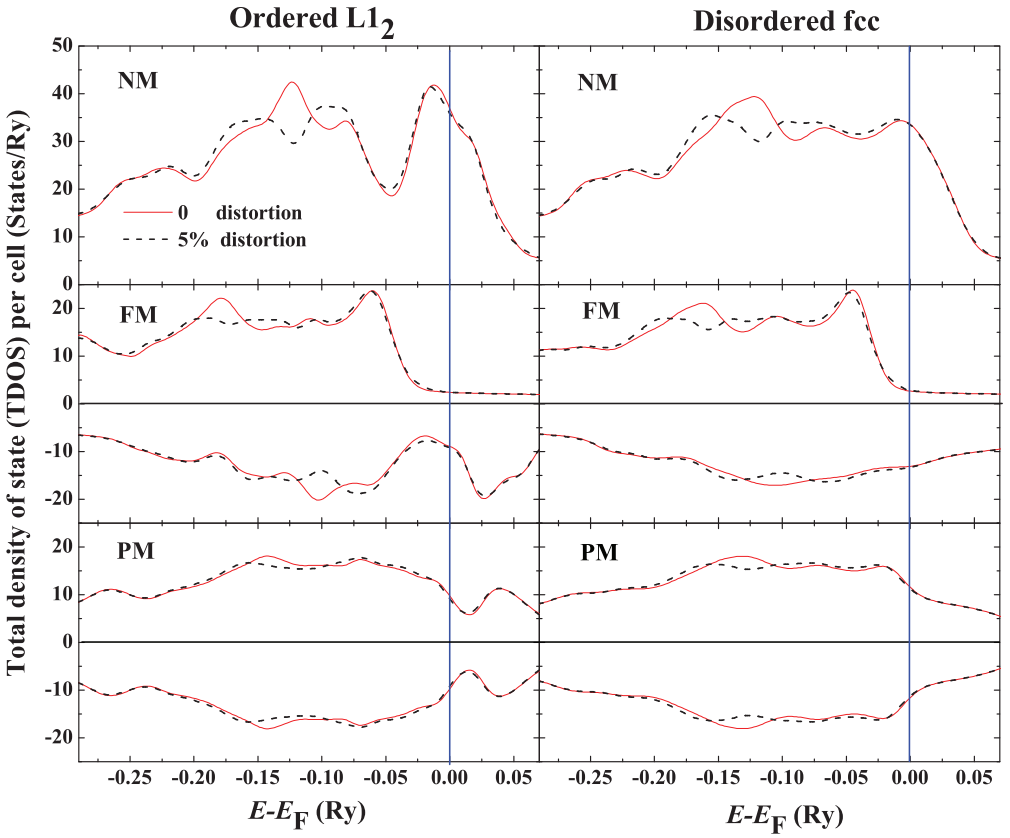

FIG. 8. (Color online) Total DOSs of NM, FM, and PM Ni_3Fe alloys for the fully ordered $L1_2$ phase (left panels) and fully disordered fcc phase (right panels). DOSs are shown for the undistorted cubic lattices (red solid curves) as well as for 5% orthorhombic distortions used to compute the tetragonal elastic constants C' (black dashed curves). The energy axis is relative to the Fermi level (E_F).

weight decreases. According to this scenario, a larger DOS peak at the Fermi level should yield a larger negative kinetic energy change (in absolute value) and hence result in a smaller elastic parameter. For instance, body-centered cubic Fe at high pressure is nonmagnetic and has a pronounced DOS peak at the Fermi level, which was used to explain the calculated large negative C' elastic parameter.[47] We should point out that the above arguments hold assuming that the systems in question possess similar electrostatic and exchange-correlation energy changes with lattice distortion. Otherwise, the force theorem fails,[48] and the latter energy terms can very well overwrite the changes dictated merely by the kinetic energy.

In the present case, we compare the ordered and disordered DOSs of various magnetic states to find the ordering effect on C'. Here we assume that the average electrostatic and exchange-correlation energy terms in $\Delta E(\delta_o)$ do not change upon chemical ordering and thus the leading energy term comes entirely from the one-electron energy (i.e., the force theorem holds). We denote by D the DOS at the Fermi level. According to Fig. 8, $D(\mathrm{NM})_{\mathrm{ord}} > D(\mathrm{NM})_{\mathrm{dis}}$ (the difference being about 3 states/Ry), suggesting $C'(\mathrm{NM})_{\mathrm{ord}} < C'(\mathrm{NM})_{\mathrm{dis}}$ based on the above scenario. Next, we find that for the spin-down channels (the spin-up channels are very similar) $D(\mathrm{FM})_{\mathrm{ord}} < D(\mathrm{FM})_{\mathrm{dis}}$ (the difference being about 5 states/Ry), indicating $C'(\mathrm{FM})_{\mathrm{ord}} > C'(\mathrm{FM})_{\mathrm{dis}}$. Finally, $D(\mathrm{PM})_{\mathrm{ord}} < D(\mathrm{PM})_{\mathrm{dis}}$ (the difference being about 1 states/Ry), resulting in $C'(\mathrm{PM})_{\mathrm{ord}} > C'(\mathrm{PM})_{\mathrm{dis}}$. Moreover, considering the relative differences between the ordered and disordered DOSs at the Fermi level, we may conclude that the difference between the ordered and disordered C''s should be largest for the FM state and smallest for the PM state. All these predictions are in perfect agreement with the actual trends from Fig. 5. It is gratifying that the above simple arguments, based merely on the total electronic density of states, can account for the fully self-consistent results.

Comparing the undistorted and distorted DOSs in Fig. 8, we can reveal some further details behind the calculated ordering effects in the C''s. The large DOS peak for ordered NM Ni_3Fe located right below E_F (near -0.015 Ry) splits upon lattice distortion. Part of it moves to energies above and part of it to energies below E_F. This results in a small decrease of $D(\mathrm{NM})$. No similar changes can be seen for the disordered NM phase, which explains why $C'(\mathrm{NM})_{\mathrm{ord}}$ is smaller than $C'(\mathrm{NM})_{\mathrm{dis}}$. On the other hand, the spin-down $D(\mathrm{FM})$ of the ordered state slightly increases with lattice distortion as a result of splitting of the DOS peaks above and below the Fermi level. Part of the local minimum is also filled up, indicating a substantial energy increase upon lattice distortion and thus a relatively large $C'(\mathrm{FM})_{\mathrm{ord}}$. For the PM state, no significant changes in the DOSs can be seen near the Fermi level, in accordance with the almost vanishing ordering effect in $C'(\mathrm{PM})$.

V. CONCLUSIONS

Using *ab initio* alloy theory, we investigated the magnetic and long-range-order effects in the elastic properties of Ni_3Fe.

For the lattice parameter a, the main effect of magnetism is concentrated in the chemically disordered region, with long-range-order parameter below $S \sim 0.6$, and the effect gradually disappears with increasing S. In the ferromagnetic state, the lattice parameter is almost constant as a function of the degree of order. Of the three single-crystal elastic constants, only C_{11} and C_{12} are found to be affected by magnetism in the ordered state; however, their combined effect results in a nearly constant bulk modulus as a function of S. C_{44} changes slightly with S and the magnetic state. The tetragonal shear modulus C', the Young's modulus E, and the shear modulus G increase significantly with the degree of order in the ferromagnetic state, but the effect becomes weak as the system approaches the random regime. In particular, the C' shear modulus depends strongly on the magnetic state and the degree of order. As a result, the Zener anisotropy C_{44}/C' and the Possion ratios are strongly affected by the long-range order in the ferromagnetic state. Nevertheless, the actual values for the Pugh ratio and the Cauchy pressure remain far from their critical values, indicating that the ductility of Ni_3Fe is not influenced by the chemical and/or magnetic ordering.

For both ferromagnetic and paramagnetic states, the chemically disordered phase is elastically softer, which contributes by $0.024k_B$–$0.147k_B$ to the ordering entropy, depending on the magnetic state. On the other hand, using a nonmagnetic approximation for the paramagnetic state, as is often done in standard density functional calculations, would result in a softer ordered phase and thus in negative ordering entropy. The calculated trends were explained using the electronic density of states of ordered and disordered nonmagnetic, ferromagnetic, and paramagnetic Ni_3Fe alloys. We showed that the details of the DOSs can fully account for the calculated ordering effects in C' and thus also in the Young's and shear moduli and Debye temperature. The present findings highlight the importance of the magnetic state in studying chemical ordering and demonstrate that the magnetic effects can overwrite the chemical terms.

ACKNOWLEDGMENTS

This work was supported by the Swedish Research Council, the European Research Council, and the China Scholarship Council. The Hungarian Scientific Research Fund (OTKA Grants No. 84078 and No. 109570) is also acknowledged for financial support.

[1] A. Kanrar and U. Ghosh, J. Appl. Phys. **52**, 5851 (1981).
[2] A. Kanrar and U. Ghosh, J. Phys. Chem. Solids **44**, 457 (1983).
[3] M. Bhatia and R. Cahn, Intermetallics **13**, 474 (2005).
[4] T. Kollie, J. Scarbrough, and D. McElroy, Phys. Rev. B **2**, 2831 (1970).
[5] Y. Himuro, Y. Tanaka, N. Kamiya, I. Ohnuma, R. Kainuma, and K. Ishida, Intermetallics **12**, 635 (2004).
[6] R. Wakelin and E. Yates, Proc. Phys. Soc., London, Sect. B **66**, 221 (1953).
[7] R. Bozorth and J. Walker, Phys. Rev. **89**, 624 (1953).
[8] C. Chinnasamy, A. Narayanasamy, N. Ponpandian, K. Chattopadhyay, and M. Saravanakumar, Mater. Sci. Eng. A **304**, 408 (2001).
[9] P. Villars and L. D. Calvert, *Pearson's Handbook of Crystallographic Data for Intermetallic Compounds*, Vol. 44073 (American Society for Metals, Materials Park, OH, 1991).
[10] A. Lutts and P. Gielen, Phys. Status Solidi B **41**, K81 (1970).
[11] L. Vitos, H. L. Skriver, B. Johansson, and J. Kollár, Comput. Mater. Sci. **18**, 24 (2000).
[12] L. Vitos, Phys. Rev. B **64**, 014107 (2001).
[13] L. Vitos, I. A. Abrikosov, and B. Johansson, Phys. Rev. Lett. **87**, 156401 (2001).
[14] L. Vitos, *Computational Quantum Mechanics for Materials Engineers: The EMTO Method and Applications* (Springer-Verlag, London, 2007).
[15] P. Soven, Phys. Rev. **156**, 809 (1967).
[16] B. Gyorffy, Phys. Rev. B **5**, 2382 (1972).
[17] E. K. Delczeg-Czirjak, E. Nurmi, K. Kokko, and L. Vitos, Phys. Rev. B **84**, 094205 (2011).
[18] G.-S. Wang, E. K. Delczeg-Czirjak, Q.-M. Hu, K. Kokko, B. Johansson, and L. Vitos, J. Phys.: Condens. Matter **25**, 085401 (2013).
[19] O. K. Andersen, C. Arcangeli, R. W. Tank, T. Saha-Dasgupta, G. Krier, O. Jepsen, and I. Dasgupta, MRS Proceedings **491** (1997).
[20] M. Zwierzycki and O. Andersen, Acta Phys. Pol. A **97**, 1 (2008).
[21] J. Kollár, L. Vitos, H. L. Skriver, and H. Dreyssé, *Electronic Structure and Physical Properties of Solids: The Uses of the LMTO Method* (Springer-Verlag, Berlin, 2000).
[22] L. Vitos, J. Kollár, and H. L. Skriver, Phys. Rev. B **55**, 4947 (1997).
[23] J. Kollár, L. Vitos, and H. L. Skriver, Phys. Rev. B **55**, 15353 (1997).
[24] A. Landa, J. Klepeis, P. Söderlind, I. Naumov, O. Velikokhatnyi, L. Vitos, and A. Ruban, J. Phys.: Condens. Matter **18**, 5079 (2006).
[25] B. Magyari-Kope, L. Vitos, B. Johansson, and J. Kollár, Acta Crystallogr., Sect. B: Struct. Sci. **57**, 491 (2001).
[26] L. Huang, L. Vitos, S. K. Kwon, B. Johansson, and R. Ahuja, Phys. Rev. B **73**, 104203 (2006).
[27] J. Kollár, L. Vitos, J. M. Osorio-Guillén, and R. Ahuja, Phys. Rev. B **68**, 245417 (2003).
[28] V. L. Moruzzi, J. F. Janak, and K. Schwarz, Phys. Rev. B **37**, 790 (1988).
[29] W. Bragg and E. Williams, Proc. R. Soc. London, Ser. A **145**, 699 (1934).
[30] J. P. Perdew, K. Burke, and M. Ernzerhof, Phys. Rev. Lett. **77**, 3865 (1996).
[31] H. Zhang, M. P. J. Punkkinen, B. Johansson, S. Hertzman, and L. Vitos, Phys. Rev. B **81**, 184105 (2010).
[32] C. Asker, L. Vitos, and I. A. Abrikosov, Phys. Rev. B **79**, 214112 (2009).
[33] H. Pitkänen, M. Alatalo, A. Puisto, M. Ropo, K. Kokko, M. P. J. Punkkinen, P. Olsson, B. Johansson, S. Hertzman, and L. Vitos, Phys. Rev. B **79**, 024108 (2009).
[34] B. L. Györffy, A. J. Pindor, J. Staunton, G. M. Stocks, and H. Winter, J. Phys. F **15**, 1337 (1985).
[35] P. A. Korzhavyi, A. V. Ruban, I. A. Abrikosov, and H. L. Skriver, Phys. Rev. B **51**, 5773 (1995).
[36] A. V. Ruban and H. L. Skriver, Phys. Rev. B **66**, 024201 (2002).
[37] A. Zunger, S.-H. Wei, L. G. Ferreira, and J. E. Bernard, Phys. Rev. Lett. **65**, 353 (1990).
[38] C. Wolverton, Acta Mater. **49**, 3129 (2001).

[39]T. Mohri and Y. Chen, J. Alloys Compd. **383**, 23 (2004).
[40]M.-Z. Dang and D. G. Rancourt, Phys. Rev. B **53**, 2291 (1996).
[41]H. Ledbetter, J. Appl. Phys. **57**, 5069 (1985).
[42]H. Siethoff and K. Ahlborn, J. Appl. Phys. **79**, 2968 (1996).
[43]P. Turchi, Y. Calvayrac, and F. Plicque, Phys. Status Solidi A **45**, 229 (1978).
[44]S. Pugh, Philos. Mag. **45**, 823 (1954).
[45]G. Grimvall, *Thermophysical Properties of Materials* (North-Holland, Amsterdam, 1999).
[46]M. Ekholm, H. Zapolsky, A. V. Ruban, I. Vernyhora, D. Ledue, and I. A. Abrikosov, Phys. Rev. Lett. **105**, 167208 (2010).
[47]K. Kádas, L. Vitos, B. Johansson, and R. Ahuja, Proc. Natl. Acad. Sci. USA **106**, 15560 (2009).
[48]H. L. Skriver, Phys. Rev. B **31**, 1909 (1985).